EXPERIMENTAL STUDY OF AEROFOIL-WAKE INDUCED TRANSITION IN BOUNDARY LAYERS

Dhamotharan Veerasamy
City University London, United Kingdom

Keywords: *Aerofoil-wake, Transition, Cylinder-wake, Flaps, Boundary layer*

Abstract

Wake induced transition in multi-element aerofoils and turbomachines are striking research problems of interest because of their influence on the aerodynamic performance. To address this problem, experimental investigations have previously been conducted to understand the interaction between a circular cylinder-wake and a flat plate boundary layer. However, the wake characteristics of the circular cylinder and the aerofoil are completely different, resulting in distinct transition mechanisms on the downstream body. In this context, the present research addresses the interaction problem considering a more realistic system involving an aerofoil and a flat plate. Further, a comparative study between aerofoil-wake and circular cylinder-wake induced transitions has been performed. In addition, free stream turbulence (FST) induced transition is also considered for comparison. Parametric studies have been conducted to study the effect of factors such as the free stream Reynolds number and the distance between the aerofoil and the flat plate in both streamwise and wall normal directions.

1 Introduction

Research on laminar–turbulent transition, initiated by Reynolds more than a century ago, is still on going. However given the nature and complexity of problem the underlying physics is not well established. Particular problems of interest are mechanism of transition and the location of transition onset. These aspects play a major role in influencing the performance of any fluid dynamic system. Understanding and thereby predicting the transition onset is still a major challenge for the aerodynamics community. One of the obvious reasons for this lack of understanding is due to influence of multiple factors on the transition onset, such as surface roughness, free stream disturbances, pressure gradients, acoustics etc.

Decades-long research investigations have addressed the above problem for a single aerodynamic surface to a reasonably successful extent. However, when it comes to a system with multiple aerodynamic surfaces (e.g. multi-element aerofoil, turbomachines) the severity of the above mentioned factors significantly increases. This, in turn, makes the physics much more complex. Because of the very nature of the problem, literature studies have addressed the issue through simplified experimental setup and computational models (e.g. Rumsey and Ying, 2002; Van Dam 2002). For instance several researchers, Mandal and Dey (2011), Pan et al. (2008), Ovchinnikov et al. (2006), kyriakides et al. (1999) have investigated the effect of circular cylinder-wake interaction with the flat plate boundary layer.

From Pan et al. (2008), it has been observed that coherent structures of the circular cylinder-wake behave largely like spanwise vortices. These spanwise vortices interact at a distance with the boundary layer of the downstream body and induce a secondary, transverse vortical structure. Secondary instability of this vortex structure leads to hairpin shaped vortices which grow with the associated streaky structures, eventually leading to fully turbulent flow.

Mandal and Dey (2011) also reported similar transition mechanisms in the cylinder-flat plate system. From these simplified experiments, yet still involving complex physics, we can infer the physics of one transition mechanism; however these results do not directly describe the transition mechanisms involved in multi-element aerofoils. This is due to the significantly different characteristics of the circular cylinder-wake and aerofoil-wakes.

We anticipate, in aerofoils at high Reynolds numbers, the coherent structures in the wakes are not like spanwise vortices, unless there is a significant flow separation. Difference in the coherent structures of the wake would result in a different transition mechanism as compared with cylinder-wake.

In addition, for the circular cylinder-wake boundary layer interaction, Mandal and Dey (2011), Pan et al. (2008) and Ovchinnikov et al. (2006) observed features of bypass transition such as self-similarity of u_{rms} profile, low and high speed streaks. Streak instability studies corresponding to FST induced transitions from Andersson et al (2001) support the observations in the circular cylinder-wake induced transition. From the literature of circular cylinder-wake boundary layer interaction, we can confirm, the onset of transition depends upon the upstream wake coherent structures but the later stage of breakdown is more like bypass transition.

As discussed in the brief literature review above, several experiments have been conducted for studying the circular cylinder-wake boundary layer interaction. However, the studies do not necessarily offer insights into more realistic wake interactions, for example in wing-flap system and turbomachinery flows. It is therefore the goal of present research to extend the scope of the above research problem considering more realistic representation of practical aerodynamic systems. From such a perspective, experimental investigations have been carried out to understand the aerofoil-wake interaction with flat plate boundary layer. Further, comparative studies between aerofoil-wake induced transition, circular cylinder-wake induced transition and free stream turbulence (FST) induced transition are conducted and the results are reported.

2 Experimental setup

The whole experiment was conducted in the low-turbulence wind tunnel at City University London, which has a test section of 0.95 x 0.91 x 4.48m with an operating velocity of 5m/s to 25m/s. Free stream turbulence intensity is below 0.01% at 15m/s. A NACA0014 aerofoil is placed upstream of a flat plate leading edge to generate the wake. To avoid vortex shedding from the aerofoil, transition trip was placed at 10% of the chord. The chord length of the flat plate and aerofoil (c) are 2.125m and 0.253m respectively. Figure 1 shows the schematic setup of the experiment, where the aerofoil is varied with four different wall normal stations (Δh) and three different streamwise stations ($\Delta x/c$).

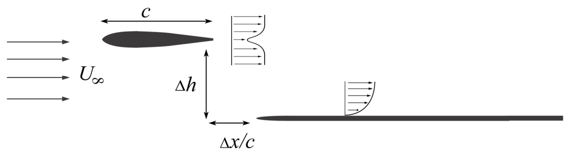

Figure 1 Schematic setup of the experiment

The experiment is performed at three different Reynolds numbers which are shown in table 1. A 55P05 Dantec boundary layer probe is used for velocity profile measurement and the signals are sampled at 10 kHz for 5 to 10 seconds with the bandpass filter of 5 Hz to 5 Hz. The aerofoil wake, when positioned at Δh = 60 or 80 mm, has no influence on the boundary layer, which can be seen clearly from figure 2 where the mean velocity profile measured over the plate is self–similar with the Blasius solution.

Case	$\Delta x/c$	Δh (mm)	Re_c ($\times 10^5$)
Case 1	0.25	20, 40, 60, 80	0.84, 1.68, 3.37
Case 2	0.5	20, 40, 60, 80	0.84, 1.68, 3.37
Case 3	0.75	20, 40, 60, 80	0.84, 1.68, 3.37

Table 1 Test cases considered in the experiment

So, for the purpose of transition studies only two wall normal stations $\Delta h = 20\ and\ 40\ mm$ are considered for analysis.

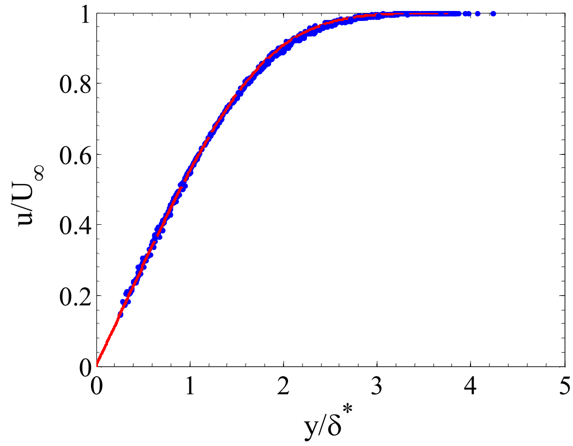

Figure 2 Self-similar velocity profile satisfying the Blasius solution for all the three cases at Δh *= 60 and 80 mm and all three* Re_c.

3. Effect on boundary layer transition due to aerofoil –wake position (Δh, $\Delta x/c$, Re_c)

Identifying the exact location of transition onset and its breakdown is one of the most critical issues in transitional research. Many intermittency methods (e.g. Zhang et al. 1995, Ramesh O. N. 1996) have been developed to identify the transition region, but their accuracy varies with the type of flow. In the present work, transition onset and its breakdown are identified by plotting skewness along the streamwise direction. For laminar flow skewness will be zero and for transitional flows skewness will have a sign reversal. At the onset of transition skewness will have a positive sign and becomes zero nearly at the intermittency of 0.5. During breakdown, skewness will have negative peak and gradually asymptotes to zero in the fully turbulent region. Figure 3 shows the skewness distribution for various streamwise location of the aerofoil.

Based on the above skewness definition in the transition region, transition onset (x_{ts}) and breakdown (x_{te}) are identified for all three cases and it is shown in table 2-4. At $\Delta h = 40\ mm$, breakdown occurs beyond the measurement regime, so only the transition onset points are shown in the table.

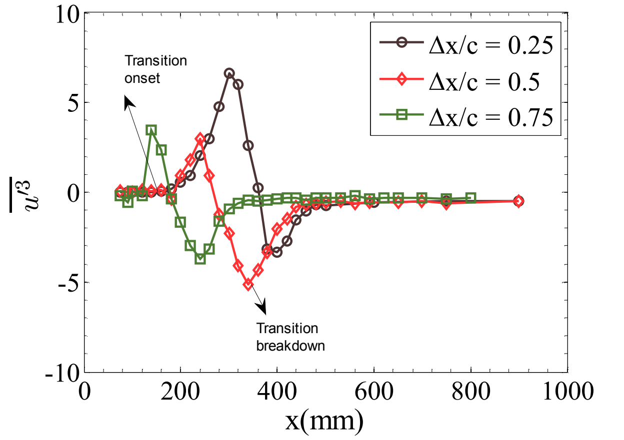

Figure 3 Skewness distribution for all three cases at $\Delta h = 20\ mm$ *and* $Re_c = 3.37 \times 10^5$

Case 1

Δh	$Re_c \times 10^5$					
	0.84		1.68		3.37	
	x_{ts}	x_{te}	x_{ts}	x_{te}	x_{ts}	x_{te}
20	280	480	260	480	180	400
40	725	---	680	---	580	---

Table 2 Transition onset and breakdown for case1, $\Delta x/c$ *= 0.25*

Case 2

Δh	$Re_c \times 10^5$					
	0.84		1.68		3.37	
	x_{ts}	x_{te}	x_{ts}	x_{te}	x_{ts}	x_{te}
20	200	480	180	440	160	340
40	850	---	725	---	680	---

Table 3 Transition onset and breakdown for case1, $\Delta x/c$ *= 0.5*

Case 3

Δh	$Re_c \times 10^5$					
	0.84		1.68		3.37	
	x_{ts}	x_{te}	x_{ts}	x_{te}	x_{ts}	x_{te}
20	200	420	100	380	75	240
40	700	---	650	---	550	---

Table 4 Transition onset and breakdown for case1, $\Delta x/c$ *= 0.75*

3.1 Effect of wall normal variation (Δh)

From the skewness distribution, it is expected that, if the wall normal gap (Δh) between the aerofoil and flat plate increases then the transition onset point shifts downstream. This is due to the fact that if the vertical gap increases then the interaction of wake disturbances with the boundary layer takes place further downstream, so that transition onset also shifts downstream. On the other hand, from figure 4, maximum energy growth along the streamwise direction is becoming steeper with increase in Δh, although with a slightly later rise. It was expected that the energy growth rate would depend on forcing disturbance and boundary layer thickness. i.e., the energy growth rate would increase with an increase in forcing disturbance or boundary layer thickness.

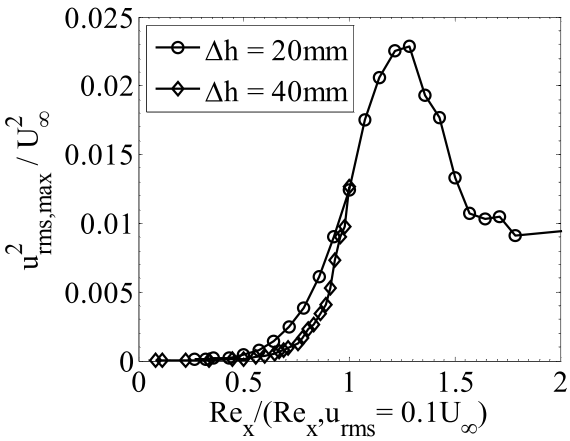

Figure 4 Maximum energy growth along streamwise direction for various Δh at $\boldsymbol{\Delta x/c} = \mathbf{0.25}$ *and* $\boldsymbol{Re_c}$ ***= 3.37 × 10***$^{\boldsymbol{5}}$.

3.2 Effect of streamwise variation ($\Delta x/c$)

An increase in the streamwise gap ($\boldsymbol{\Delta x/c}$) causes earlier transition onset on the flat plate, which can be seen clearly from figure 3. The cause of this effect is assumed to be due to the earlier interaction of the wake with the boundary layer, because of the increase in wake thickness upstream of the flat plate. However, as the wake develops downstream, the intensity of the turbulence in the wake will reduce. Due to the reduced strength of the forcing and to the reduced boundary layer thickness at transition onset, the disturbance growth rate following transition onset will be reduced. Figure 5 clearly shows the normalized energy growth rate along the streamwise direction reduces with the increase in streamwise gap.

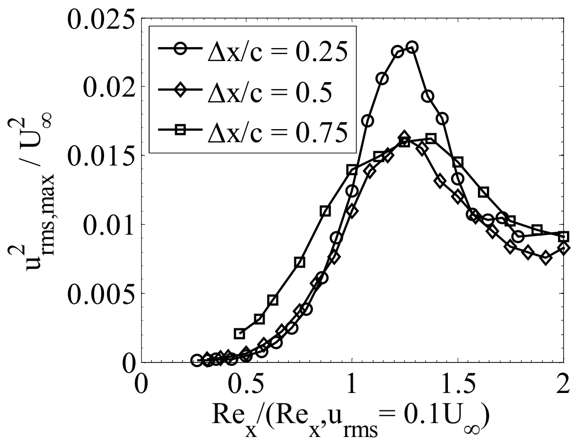

Figure 5 Maximum energy growth along streamwise direction for various $\Delta x/c$ at $\boldsymbol{\Delta h} = \mathbf{20}\ \boldsymbol{mm}$ and **Re$_c$ = 3.37 × 10^5**.

3.3 Effect of Reynolds number ($\boldsymbol{Re_c}$)

It is apparent that the increase in Reynolds number increases the turbulence level in the wake, which causes earlier transition on the flat plate. Also, increase in disturbance level should increase the energy growth rate and that is confirmed from figure 6.

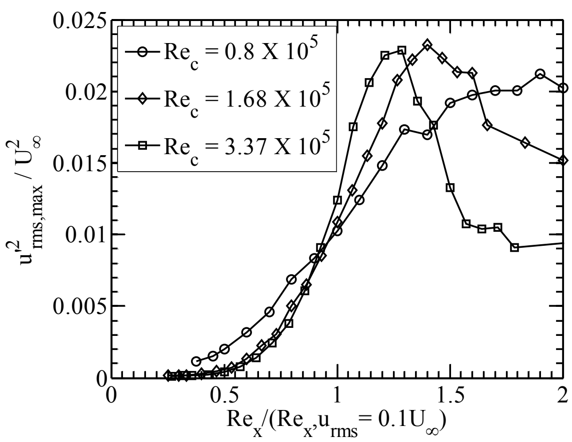

Figure 6 Maximum energy growth along streamwise direction for various Re_c at $\boldsymbol{\Delta h} = \mathbf{20}\ \boldsymbol{mm}$ and $\boldsymbol{\Delta x/c} = \mathbf{0.25}$.

4. Comparative study with circular cylinder-wake and FST induced transition.

In this section the energy distribution for aerofoil-wake induced transition is compared with circular cylinder-wake induced transition and FST induced transition. Data from Mandal and Dey (2011) and Ovchinnikov et al (2006) is used as the reference case for circular cylinder-wake induced transition. For FST-induced transition the results of Fransson et al (2005) are considered for comparison.

We note that the various experimental conditions reported in the literature are not the same, nor are they for the present experiment. Fortunately, the linear growth of the disturbance energy obtained from different measurement conditions in the literature does collapse onto a single curve, as seen in Mandal and Dey (2011) and Fransson et al (2005). So, here we hope to verify whether the linear growth of the disturbance energy obtained from aerofoil-wake induced transition under different measurement conditions also collapses to a single curve.

4.1 Disturbance energy growth for different Reynolds number (Re_c)

Figures 7a and 7b compare the normalised streamwise disturbance energy growth for aerofoil-wake induced transition with the circular cylinder-wake induced transition for two different Reynolds numbers at $\Delta \boldsymbol{h}$ = 20 mm. At low Reynolds number, as figure 7a clearly shows, the growth rate of the disturbance energy for aerofoil-wake induced transition is lower than for the circular cylinder-wake induced transition. On the other hand at high Reynolds number (figure 7b) the disturbance energy growth rates are same for both cases.

Normalised energy growth of the streamwise disturbance for the case of FST-induced transition is compared with aerofoil-wake induced transition in figures 8a and 8b.

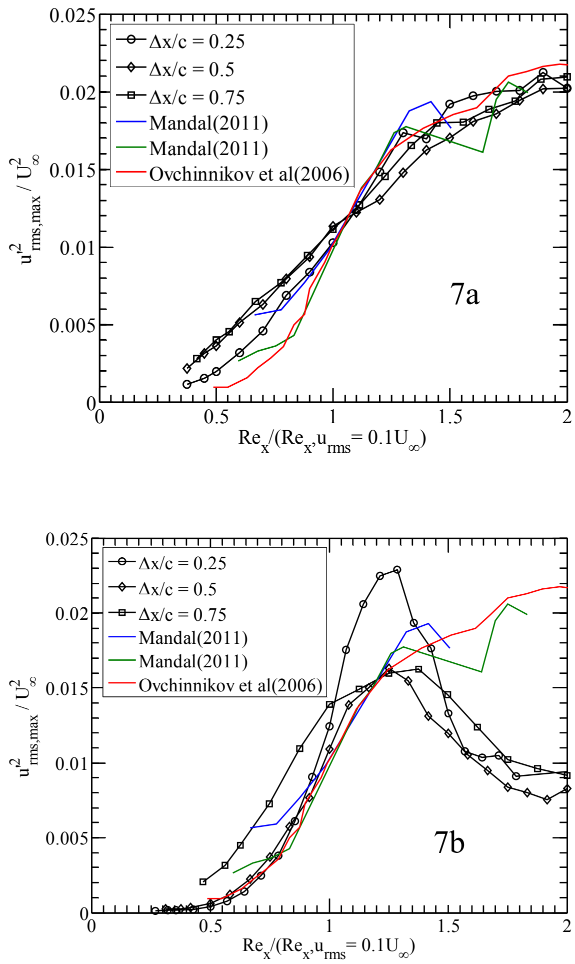

Figure 7 Comparison of streamwise growth of the disturbance energy between aerofoil-wake induced transition (lines with marker) and circular cylinder-wake induced transition (colour lines). (a)Present measurement at Δh = 20 *mm and* $\boldsymbol{Re_c} = \boldsymbol{0.8 \times 10^5}$, (b) Δh = 20 *mm and* $\boldsymbol{Re_c} = \boldsymbol{3.37 \times 10^5}$.

In contrast to the comparison of circular cylinder-wake induced transition, streamwise growth of the disturbance energy for FST-induced transition follows the same trend as the aerofoil-wake induced transition at low Reynolds number. At high Reynolds number, normalised energy growth for aerofoil-wake induced transition is steeper than for FST induced transition.

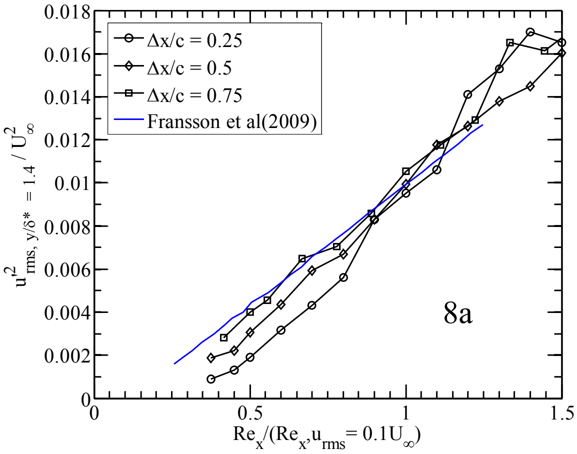

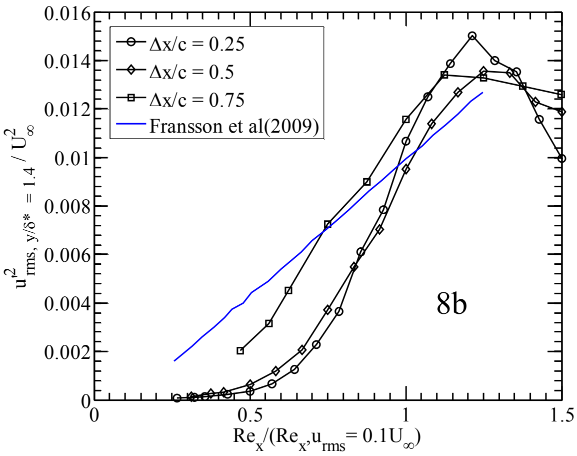

Figure 8 Comparison of streamwise growth of the disturbance energy between aerofoil-wake induced transition (lines with markers) and FST induced transition (blue line). (a) Present measurement at $\Delta h = 20$ *mm and* $\boldsymbol{Re_c = 0.8 \times 10^5}$*. (b) Present measurement at* $\Delta h = 20$ *mm and* $\boldsymbol{Re_c = 3.37 \times 10^5}$

Comparing figure 7 with figure 8 we can confirm that the normalised growth of the disturbance energy for aerofoil-wake induced transition and for circular cylinder-wake induced transition are similar at high Reynolds number. Conversely, at low Reynolds number, the normalised energy growth for FST-induced transition and for aerofoil-wake induced transition are similar.

4.2 Disturbance energy growth for different Wall normal stations (Δh)

Next, the streamwise growth of the disturbance energy, measured at $\Delta h = 20$ and 40 mm for $Re_c = 3.37 \times 10^5$ is considered, to compare the aerofoil-wake induced transition, circular cylinder-wake induced transition and FST-induced transition cases.

From figures 7b and 9, at $\Delta h = 20\ mm$, the slope of the streamwise growth of the disturbance energy for aerofoil-wake induced transition remains similar to that for the circular cylinder-wake induced transition. On the contrary, if Δh rises to 40 mm, then the energy growth for aerofoil-wake induced transition becomes steeper.

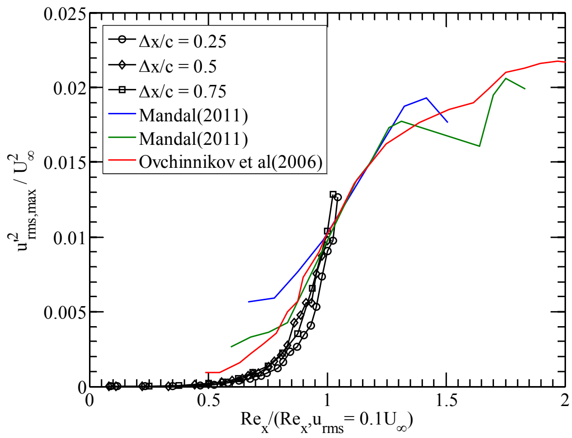

Figure 9 Comparison of streamwise growth of the disturbance energy between aerofoil-wake induced transition (lines with marker) and circular cylinder-wake induced transition (colour lines). Present measurement at $\Delta h = 40$ *mm and* $Re_c = 3.37 \times 10^5$*.*

Figures 8b and 10 show that the streamwise growth of the disturbance energy for aerofoil-wake induced transition is always steeper in comparison with the FST-induced transition case, irrespective of variation in Δh.

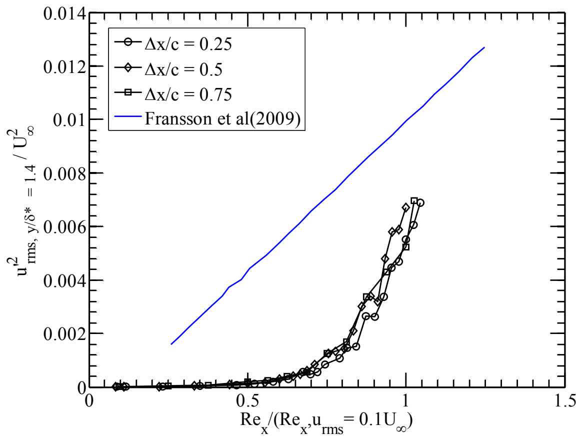

Figure 10 Comparison of streamwise growth of the disturbance energy between aerofoil-wake induced transition (lines with marker) and FST induced transition (blue line). Present measurement at $\Delta h = 40$ mm and $Re_c = 3.37 \times 10^5$.

5. Conclusion

Both transition onset and streamwise growth rates of the disturbance energy have been analysed as aerofoil-wake proximity (both Δx and Δh) and Re_c are varied. It is concluded that the transition onset point is depends on wake proximity while energy growth in the boundary layer depends on strength of the wake disturbances and the boundary layer thickness at the point of interaction. For example we consider three cases, A, B and C, shown in table 5.

Cases A and C are for the same wall normal distance (Δh) but for different streamwise offsets ($\Delta x/c$). The thickness of the wake above the boundary layer will be larger for case C than case A, due to wake growth in the downstream direction. The larger wake thickness in case C will affect the boundary layer much earlier than in case A, resulting in earlier transition in case C. On the contrary, the turbulence intensity in the wake will be higher in case A than in case C. The higher forcing level leads to more rapid transition, which can be seen clearly from figure 5 were the disturbance growth of case A is steeper than for case C.

Cases	Δh (mm)	$\Delta x/c$	$Re_c \times 10^5$
A	20	0.25	3.37
B	40	0.25	3.37
C	20	0.75	3.37

Table 5: Cases considered for analysis

Furthermore, considering cases A and B with the same $\Delta x/c$ but different Δh: case B is positioned at larger Δh, resulting in later transition onset. However the boundary layer thickness at transition for case B will be larger than for case A. The thicker boundary layer appears to give rise to an elevated disturbance growth for case B, shown in figure 4.

In addition, a comparative study between aerofoil-wake induced transition and circular cylinder-wake induced transition has been carried out for different Re_c and Δh. It is concluded that, at high Reynolds number and lower value of Δh, the energy growth of the circular cylinder and aerofoil wake cases are similar. Similarly, results from the aerofoil wake experiments are compared with FST-induced transition: at low Reynolds number, the normalised energy growth rates for FST-induced transition and aerofoil wake-induced transition are similar.

These results confirm that the length of the transition region and the streamwise disturbance growth in the boundary layer share some of the characteristics of cylinder-wake and FST-induced transition, depending upon the Reynolds number and separation of the wake. Further work will explore the reasons for the change-over in trends as these parameters are varied..

Acknowledgements

I would like to acknowledge the support of InnovateUK under grant ref. 113024, Enhanced Fidelity Transonic Wing, led by Airbus.

References

1.) Andersson, Paul, et al. "On the breakdown of boundary layer streaks."*Journal of Fluid Mechanics* 428 (2001): 29-60.

2.) Fransson, Jens HM, Masaharu Matsubara, and P. Henrik Alfredsson. "Transition induced by free-stream turbulence." *Journal of Fluid Mechanics* 527 (2005): 1-25.

3.) Kyriakides, N. K., et al. "Aspects of flow structure during a cylinder wake-induced laminar/turbulent transition." *AIAA journal* 37.10 (1999): 1197-1205.

4.) Mandal, A. C., and J. Dey. "An experimental study of boundary layer transition induced by a cylinder wake." *Journal of Fluid Mechanics* 684 (2011): 60-84.

5.) Ovchinnikov, Victor, Meelan M. Choudhari, and Ugo Piomelli. "Numerical simulations of boundary-layer bypass transition due to high-amplitude free-stream turbulence." *Journal of Fluid Mechanics* 613 (2008): 135.

6.) Pan, Chong, Wang, J. J., Zhang, P. F., & Feng, L. H. "Coherent structures in bypass transition induced by a cylinder wake." *Journal of Fluid Mechanics* 603 (2008): 367-389.

7.) Ramesh, O. N., J. Dey, and A. Prabhu. "Transitional intermittency distribution in a three-dimensional constant pressure diverging flow." *Experiments in fluids* 21.4 (1996): 259-263.

8.) Rumsey, Christopher L., and Susan X. Ying. (2002) Prediction of high lift: review of present CFD capability." *Progress in Aerospace Sciences* 38.2, 145-180.

9.) Van Dam, C. P. (2002) "The aerodynamic design of multi-element high-lift systems for transport airplanes." *Progress in Aerospace Sciences* 38.2 101-144.

10.) Zhang, D. H., Y. T. Chew, and S. H. Winoto. "A proposed intermittency measurement method for transitional boundary layer flows." *Experiments in fluids* 19.6 (1995): 426-428.

Copyright Statement

Contact Author Email Address

dhamotharan.veerasamy.1@city.ac.uk